# MODEL ANALYSIS AND EXPERIMENTAL STUDY ON MECHANICAL BEHAVIOR OF BURIED DUCTILE IRON PIPELINES SUBJECTED TO LARGE GROUND DEFORMATIONS

Shiro Takada (1)

## SUMMARY

This paper proposes a model to analyze the behavior of buried ductile cast iron pipelines subjected to large ground deformations as the first stage to build up design procedures in due consideration of ground failures. And also physical test data on mechanical behavior of the buried pipelines are given, which were done by a new test fixture designed for conducting a test with a simulation of actual large ground deformations during strong earthquakes. Simulation results have proved that appropriate soil resistant constants in the analytical model can elucidate experimental values.

## INTRODUCTION

Seismic resistant designs of buried pipelines during strong earthquakes should focus on ground failure such as faulting, liquefaction, landsliding and seismic compaction. State-of-the-art design procedures exist to quantity the ground motions for wave propagations with non-ground failure. On May 26th, 1983, a magnitude-7.7 earthquake occurred in Akita Prefecture about 500 Km NNE of Tokyo. Damage investigations of severely damaged area at Noshiro City in Akita Prefecture for gas and water pipelines revealed that over 90 % of the total number of pipe breaks were damaged due to liquefaction and permanent ground displacements followed liquefaction (Ref.1).

The present paper proposes a model to analyze the behavior of buried ductile cast iron pipelines subjected to large ground deformations as the first stage to build up design procedures in due consideration of ground failures. Besides, the present paper also gives new physical test data on mechanical behavior of buried ductile cast iron pipelines with joints subjected to large ground deformations. A test fixture has been designed for conducting test with a simulation of actual large ground deformations during strong earthquakes. Test results were then simulated by using the proposed analytical model.

## MODEL AND ANALYTICAL PROCEDURE OF BURIED PIPELINE SUBJECTED TO LARGE GROUND DEFORMATION

Models were formed to analyze buried pipelines subjected to fault movements or ground subsidence by seismic loadings as shown in Fig.1(a). Loading rates are thought to be relatively slow for buried pipelines such that the effects of inertia and damping forces may be neglected and quasi-static analysis can give adequate computational results. Soil-pipeline interaction was modeled such that a buried pipeline is a series of segmented elastic beams connected longitudinally with non-linear rotation and expansion joints; and each beam is supported by continuous ground springs with slip characteristics as shown in Fig.1

(1) Associate Professor, Civil Eng., Kobe University, Rokkodai Nada, Kobe, JAPAN

(b). One axial and one transverse vertical motions of the pipeline were analyzed. Arbitrary permanent ground deformations along the pipeline such as fault and subsidence were imposed to the buried pipeline through the ground spring.

For the segmented pipes, following equations of motion can be written for longitudinal and transverse movements.

$$-EAd^2u/dx^2 = k_u(U-u), \quad EId^4v/dx^4 = k_v(V-v) \tag{1}$$

where, E is Young's modulus of the pipe material, A and I are cross sectional area and geometrical moment of inertia of the pipe, $k_u$ represents the side resistance along the pipeline and $k_v$ represents the resistance offered by the surrounding soils to vertical translation of the pipeline. u and v are pipe deformations for longitudinal and transverse motions respectively. U and V in Eq.(1) indicate arbitrary permanent ground deformations along the segmented pipes. Fault movements and/or ground subsidence may be expressed by the mathematical forms of U and V. Fig.2(a) shows the amount of axial restraint or load exerted on the pipeline related with the amount of relative soil-pipeline displacements. Beyond a certain relative displacement $u_e$, the axial restraint by friction forces is a constant value. Fig.2(b) shows the similar relationship between transverse restraint and relative displacements. For this case, vertical movement of the buried pipeline is resisted in a different manner. The uplift resistance of the soil is much lower than the downward resistance. The values of $k_u$ and $k_v$ in Eq.(1)are given by the inclination angles of tangent lines which touch the curves shown in Fig.2(a) and (b). By integrating Eq.(1), the physical quantity $V_k^R$ of the right hand side of the k-th segmented beam can be related with the physical quantity $V_k^L$ of the left hand side of the k-th beam as

$$V_k^R = F_k \cdot V_k^L \tag{2}$$

$$V_k^{R(L)} = [u,v,\phi,M,N,Q,1]_k^{R(L)} \tag{3}$$

Here, $\phi$ is deflection angle, M, N and Q are bending moment, axial force and shear force at the end of the right and/or left hand sides of the k-th segmented beam. $F_k$ is called to be a field matrix of the k-th beam, having a function of transfering the state vector $V_k$ at one end to the other end of the beam.

The segmented beams were connected by mechanical joints. Resistance of ductile iron pipelines to large ground deformations may be restrained by the rotation and expansion capacities of the mechanical joints. Good jointing techniques will allow the buried pipelines to rotate or expand without leakage or failure even for large ground deformations. Equilibrium state of deformations and forces at joints were modeled as shown in Fig.3. Deformation and force at the right hand end of the k-th beam can be related with those at the left hand end of the (k+1)-th beam by the following equations.

$$\begin{bmatrix} u \\ v \\ \phi \end{bmatrix}_{k+1}^{L} = \begin{bmatrix} u \\ v \\ \phi \end{bmatrix}_{k}^{R} + \begin{bmatrix} -N/k_T \\ -M/k_R \\ 0 \end{bmatrix}_{k}^{R}, \quad \begin{bmatrix} N \\ M \\ Q \end{bmatrix}_{k+1}^{L} = \begin{bmatrix} N \\ M \\ Q \end{bmatrix}_{k}^{R} \tag{4}$$

where $k_T$ and $k_R$ are the translational (longitudinal) and rotation springs representing mechanical features of the joints. One example of mechanical characteristics of the joint of ductile iron pipelines, called for GM-II (Gas Mechan-

ics), is shown in Fig.4(a) for longitudinal motions and Fig.4(b) for transverse motions. Circles in the figures indicate experimental results (Ref.2) and rigid lines are idealized qualification for computations. The GM-II joints have such characteristics that the pulling out of the joint is prevented at a reach of 18 mm by the rock ring and a less margin of 5 mm is allowed for pushing in. The values of $k_T$ and $k_R$ in Eq.(4) can be given by inclination angles of each rigid line in Fig.4. Eq.(4) constitutes of the next relationship with the aid of a point matrix $P_k$ which related the state vector $V^L_{k+1}$ with $V^R_k$.

$$V^L_{k+1} = P_k \cdot V^R_k \tag{5}$$

Combining Eq.(2) with Eq.(5), we obtain the following formula:

$$V^L_{k+1} = P_k \cdot F_k \cdot V^L_k \tag{6}$$

Following the same procedure as Eq.(6), the state vector at the right hand end of the N-th beam where the boundary conditions are given, can be calculated using the $A^L_1$, the unknown state vector at the left hand end of the first segmented beam. The next linear equation can be obtained.

$$R' \cdot F_N \cdot P_{N-1} \cdot F_{N-1} \cdots\cdots P_1 \cdot F_1 \cdot R \cdot A^L_1 = 0 \tag{7}$$

where, R represents the boundary matrix which has a function to convert the unknown state vector $A^L_1$ into the generalized state vector $V^L_1$ and R' has a function to convert $V^R_N$ into the known state vector by given boundary conditions. Eq.(7) gives the solution for $A^L_1$ and then all unknown variables can be obtained with the aid of the field and point matrices. A numerical computation technique for non-linear behavior of the surrounding soil and joint springs is the load increment method to assume the behavior of the system to be linear within a certain range of the input displacements. Then, Eq.(7) is still valid for non-linear computations. Step-by-step-substitution technique and non-dimensional variables were employed to avoid the decrease of computational accuracy stemmed from multiplication of many field and point matrices.

## TEST ON MECHANICAL BEHAVIOR OF BURIED DUCTILE CAST IRON PIPELINES SUBJECTED TO LARGE GROUND DEFORMATIONS

A test fixture has been designed for conducting test with a simulation of actual large ground deformations. Fig.5 shows a sketch of the fixture (Sinking Soil Box) 10 m long (4 m fixed and 6 m movable parts), 100 cm wide and 150 cm deep. The movable part of the fixture was supported by six jacks with a vertical clearance of 200 mm. Two kinds of pipelines (CASE A and CASE B) were tested as shown in Fig.6. The pipelines in CASE A has a 984 cm total length with 3 segments of ductile iron pipes linked by two GM-II joints and in CASE B, a 918 cm total length with 5 segments linked by the same 4 joints. Different joint arrangement between CASE A and CASE B will clarify the joint efficiency to resist against the large ground deformations. Table 1 indicates dimensions and material constants of the tested pipes. Mechanical characteristics of the GM-II joint were shown in Fig.4. As shown in Fig.6, strain gauges, tilt meters for measuring joint rotation angle and displacement meter for joint expansion and compression were set up. Piano wires were used for observing vertical levels of the buried pipelines from the ground surface. The GM-II pipelines was placed on a sufficiently compacted sand soil layer of 400 mm thickness and then covered

by an 800 mm sand soil layer over the crown of the cross section of the pipe. Compaction of the soil layer was performed by using a gasoline-engine compactor. A few tests for soil characteristics were performed for sand soil specimens sampled at 300 mm beneath the ground surface. Water ratio were 13-14 % both for CASE A and CASE B. A loading test was carried out by utilizing a circular steel plate 300 mm in diameter and 30 mm thick to obtain soil stiffness. Loading test results gave the soil spring constants per unit length along the stretch of the pipelines as 30-60 kg/cm$^2$. Ground deformations (relative displacements between the fixed and movable soil boxed in Fig.5) were performed by statically winding the supporting screw jacks downwards. The total ground deformations were completed by succeeding steps of lowering of jacks. At each step of ground deformation, hoop and axial pipe strains, joint displacements, joint rotation angles and levels of the pipeline were measured.

## TEST RESULTS AND SIMULATION OF PIPELINE BEHAVIOR BY PROPOSED ANALYTICAL MODEL

Measured transverse (hoop) pipe strains were much less than longitudinal (axial) pipe strains due to bending pipe deformation. Fig.7 shows axial pipe strain distributions along the longitudianl direction of the pipeline respectively for CASE A and CASE B. The strain is an axial strain induced by 180 mm ground vertical deformation and followed by pipe bendings. Strains in CASE A are concentrated to the longest segmented pipe subjected to ground deformation and the maximum value of the strain reaches to 2000 μ. On the other hand, strains in CASE B are successfully distributed to two segmented pipes with the aid of good arrangement of GM-II joints. The maximum values of the strains are not more than 350 μ. The maximum pipe stress $\sigma_1$ at point 7 designated in Fig.6 are related with ground deformation for CASE A and CASE B in Fig.8. The stress is calculated by the following equations:

$$\sigma_1 = E(\varepsilon_1+\nu\varepsilon_2)/(1-\nu^2), \quad \sigma_2 = E(\varepsilon_2+\nu\varepsilon_1)/(1-\nu^2) \tag{8}$$

where, $\sigma_1$ and $\sigma_2$ are axial and hoop stresses, $\varepsilon_1$ and $\varepsilon_2$ are measured axial and hoop strains, E and $\nu$ are Young's modulus and Poisson's ratio for ductile iron pipe materials. For CASE A , the maximum stress increases linearly according to an increase of the ground deformation and 15 cm of the ground subsidence is considered to be allowable value registed by the ductile iron pipe materials. On the contrary, the rate of increase of the maximum pipe stress in CASE B are much less than that of CASE A, because the pipeline deforms following the ground distortions owing to successful joint arrangement. Buried pipelines with shorter joint distance like CASE B may be susceptible to larger ground deformations. Fig.9 is the data on joint extraction behavior in accordance with an increase of the ground deformation for CASE A and CASE B. The amount of joint extraction is scanty for both cases compared with an allowable extraction value of 60 mm in GM-II joint. Abnormally high values of No.2 joint extraction observed at the ground subsidence of 80-90 mm in CASE B are thought to be some effects of ground failures, where soil cracks started to come out in the ground surface over the No.2 joint. In other words, the joint become easy to be extracted due to decrease of soil resistances around the joint by outbreaking of soil cracks. Joint rotation characteristics are shown in Figs.10 and 11. The maximum rotation angle of 3 degrees for CASE A and CASE B is not so small value campared with an allowable rotation angle of 7-8 degrees in GM-II joints. The rotation angles in CASE A have linear relation with an increase of the ground deformations. However, the behaviors of No.2 and No.3 joints in CASE B are not so simple as shown in Fig.11. A high value of the

rotation angle at No.2 joint in CASE B were measured for the 80-90 mm ground subsidence because of the same reason as the case of the joint extraction behavior. Judging from the signs of the joint rotation angles in CASE B, a 50 mm ground subsidence demarcates the features of the pipeline deformations. Fig.12 shows one example of the pipeline deformation and the joint rotation angle for smaller or larger ground subsidence. Test results gave lessons that joint rotation characteristics and joint arrangements are much more important factors than joint extraction characteristics for such as uplift and downward large deformations.

Computer simulations were carried out for experimental buried pipeline models, CASE A and CASE B by employing the procedures proposed in the previous section. Pipe dimensions and materials listed in Table 1 and the GM-II joint characteristics shown in Fig.4 were introduced for numerical computations. As for the soil resistant constants $k_u$ and $k_v$ in Eq.(1), next relations were adopted following Reference (3).

$$k_u = k_v = \pi k D \tag{9}$$

here, D is pipe diameter and k is a constant value. Values of $k_u$ and $k_v$ are most sensitive to the analytical results among computational parameters. The distribution of k values along the longitudianl direction of the pipeline model shown in Fig.13 turns out to be most suitable to explain the experimental results for both CASE A and CASE B. To say, the soil spring constants in the fixed ground have much larger values than that of the subsiding ground. Figs.14 and 15 show simulated stress distributions along the pipeline axis for several steps of the ground subsidence on CASE A and CASE B. Distribution configurations and amounts of pipe bending stresses in the figures do not conflict with the experimental results shown in Figs.7 and 8. Simulated joint rotation angles related with the ground subsidence for CASE A and CASE B are also plotted in Figs.10 and 11. The simulated value gives good comparisons with the experimental one except for the abnormal high values of rotation angles due to ground failures. Simulated pipe deformations for CASE A and CASE B were compared with measured deformations in Fig.16. Computational results prove that appropriate soil resistances in the model analysis can elucidate the values measured in the experiments.

## REFERENCES


(1) Takada,S., Tanabe,T. and Fudaki,H. "Report on Pipe Damages during 1983 Akita-Ken-Oki Earthquake," July 1983.

(2) Osaka Gas Company Ltd. "Experiments on Joint Characteristics," Osaka Gas Report, December 1981.

(3) Toki,K., Fukumori,Y., Sako,M. and Tsubakimoto,T. "Recommended Practice for Earthquake Resistant Design of High Pressure Gas Pipelines," PVP-77, June 1983, pp.349-356.

Table 1 Dimensions of Pipe

| | |
|---|---|
| Diameter (mm) | 169 |
| Thickness (mm) | 8.5 |
| Poisson's Ratio | 0.35 |
| Young's Modulus ($kg/cm^2$) | $1.6 \times 10^6$ |

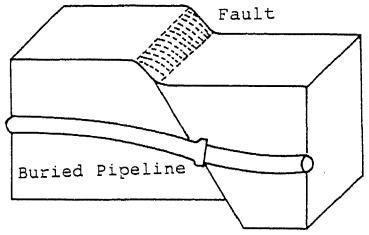


Fig.1(a) Actual Geology

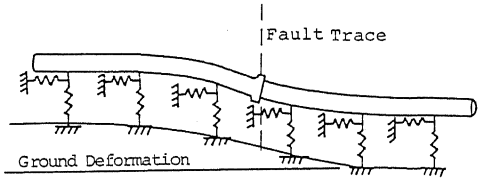


Fig.1(b) Analytical Model

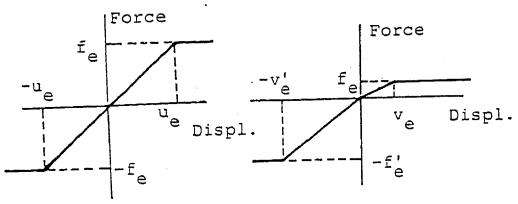


(a) Longitudinal (b) Transverse

Fig.2 Soil Restrint

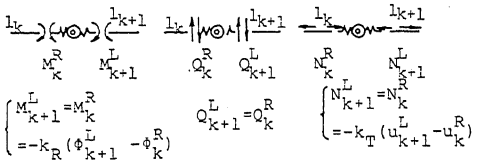


Fig.3 Analytical Joint Model

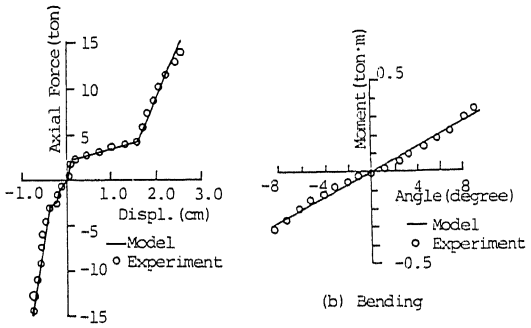


(a) Axial Force (b) Bending

Fig.4 Joint Characteristics (GM-II)

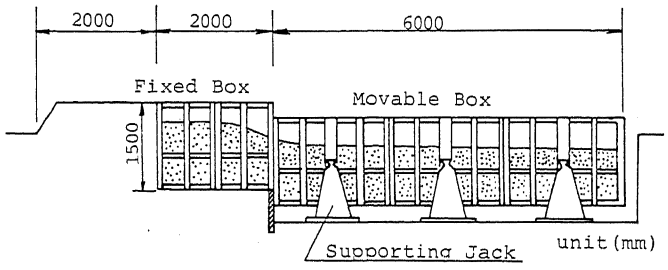


Fig.5 Test Fixture

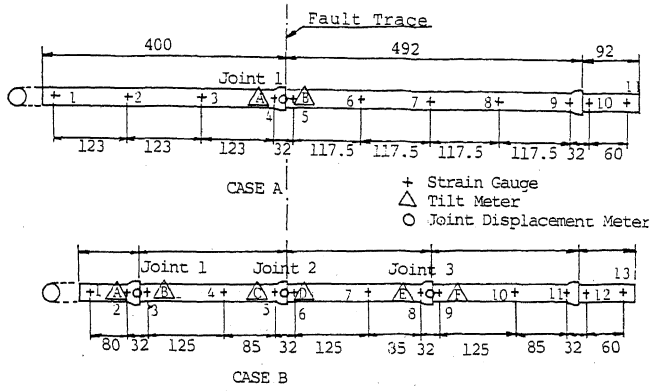


Fig.6 Tested Pipelines and Measured Points

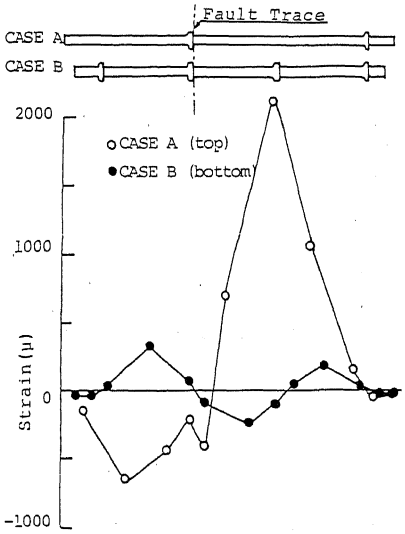


Fig.7 Measured Pipe Strain

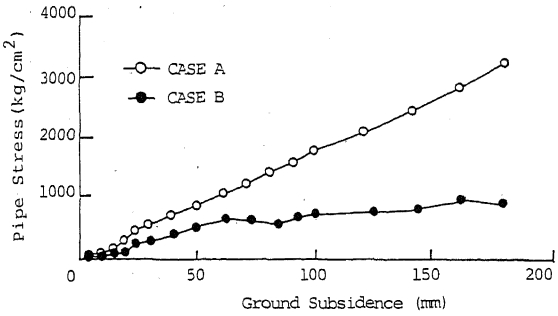


Fig.8 Maximum Pipe Stress Related with Ground Subsidence

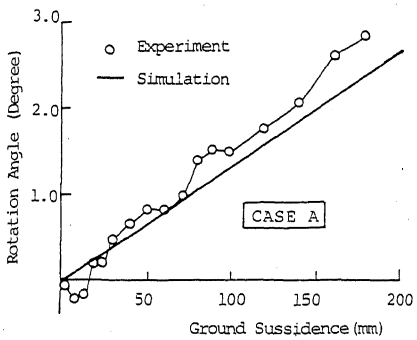


Fig.10 Joint Rotation Angle Related with Ground Subsidence

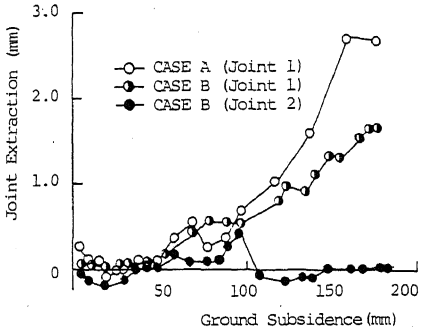


Fig. 9 Joint Extraction Related with Ground Subsidence

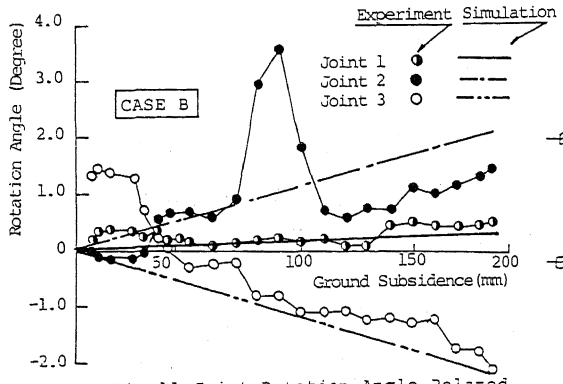


Fig.11 Joint Rotation Angle Related with Ground Subsidence

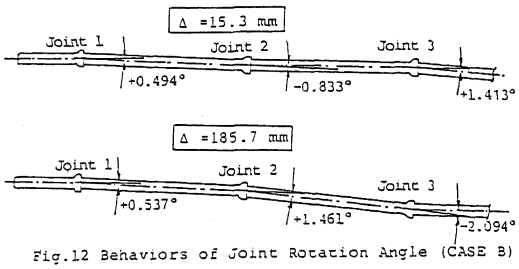


Fig.12 Behaviors of Joint Rotation Angle (CASE B)

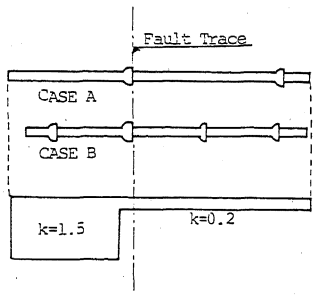


Fig.13 Optimum Coefficients for Soil Resistance

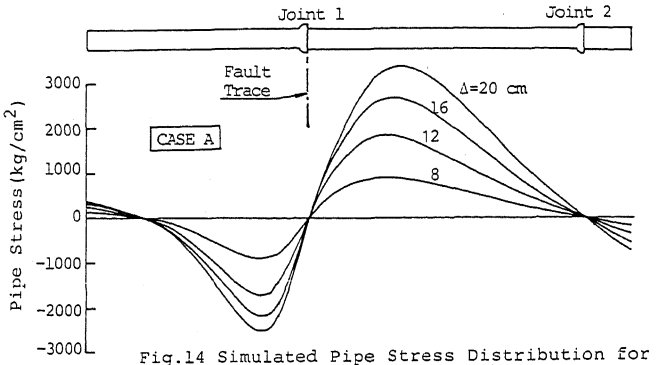


Fig.14 Simulated Pipe Stress Distribution for Different Ground Subsidence

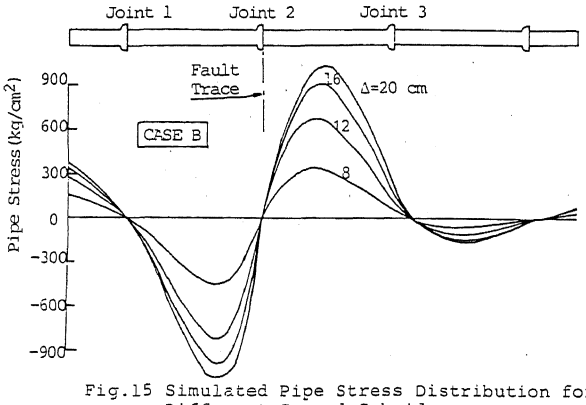


Fig.15 Simulated Pipe Stress Distribution for Different Ground Subsidence

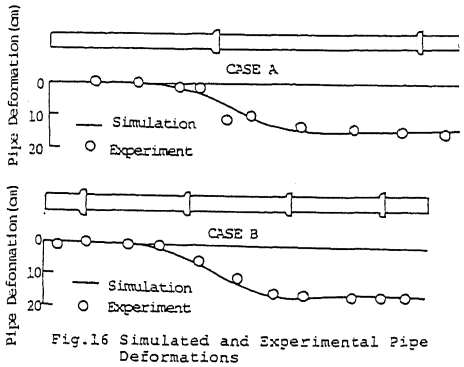


Fig.16 Simulated and Experimental Pipe Deformations